INTERPRETATION OF FLUORESCENCE DECAYS IN PROTEINS USING CONTINUOUS LIFETIME DISTRIBUTIONS

J. RICARDO ALCALA, ENRICO GRATTON, AND FRANKLIN G. PRENDERGAST*
Physics Department, University of Illinois at Urbana-Champaign, Urbana, Illinois 61801; and
**Department of Biochemistry and Molecular Biology, Mayo Foundation, Rochester, Minnesota 55905*

ABSTRACT The decay of the tryptophanyl emission in proteins is often complex due to the sensitivity of the tryptophan excited state to its surroundings. The traditional analysis of the decay curve using exponential components is based on the identification of each component with a particular protein conformation. An alternative approach assumes that proteins can exhibit a large number of conformations and that, at room temperature, the interconversion rate between conformations can be of the same order of magnitude as the excited-state decay rate. Following this assumption, the analysis of the protein emission was performed using continuous distributions of lifetime values. The number of average protein conformations, the range of mobility around each conformation, and the rate of interconversion between conformations determines the characteristics of the lifetime distribution. The fluorescence decay from some single tryptophan proteins was measured using multifrequency phase fluorometry and analyzed using a sum of exponentials, unimodal and bimodal probability-density functions, and the analytical form for lifetime distribution obtained for a model in which the tryptophan residue can move in a single potential well. For ribonuclease T1 and neurotoxin variant 3, the sum of two exponentials and bimodal probability-density functions gave comparable results, whereas for phospholipase A2, the description of the decay required three exponentials or bimodal probability-density functions. Also the temperature dependence of the fluorescence decay was investigated. It was found that the lifetime distribution was broader and shifted toward longer lifetime values at lower temperature. The analysis of the decay of tryptophan in buffer and of some tryptophan derivatives gave single-exponential decays. The single-potential well lifetime distribution, which has only three adjustable parameters, gave good fits for all cases investigated, but in the case of phopholipase A2, the temperature dependence of the parameters that describe the single-potential well distribution indicated the inadequacy of this model at lower temperature, suggesting that multiple potential wells can describe better the decay for this protein.

INTRODUCTION

The sensitivity of the excited state of a fluorophore to the physicochemical properties of its environment is a major reason why fluorescence techniques are so frequently used to study protein structure and function. However, this self-same sensitivity frequently makes the signals too complex to be interpreted simply, irrespective of the fluorescence property being measured. Of all the fluorescence parameters that can be measured, the fluorescence lifetime is often the most problematic to interpret as it is subject to perturbation by both mechanical and physicochemical factors and it is often difficult or impossible to identify the perturbants unequivocally in a macromolecule. However, fluorescence lifetime values are highly sensitive to the particular environment. In a recent review (1) it is reported that the lifetime of the tryptophanyl residue varies by more than of a factor of 100 in different proteins. Also it is well established that protein structural fluctuations can occur in the nanosecond–picosecond time scale (2–5). It is legitimate to believe that these rapid fluctuations would affect the lifetime value. Furthermore, it has become apparent that the interpretation of particular fluorescence lifetime values in terms of water accessibility to, or location of a fluorophore in a protein often cannot be justified, and that generalized inferences regarding protein structure made from such data may be invalid.

More recently, it has been proposed that even the traditional approach to interpretation of fluorescence lifetimes, per se, may be suspect (6, 7). For example, we have grown accustomed to interpreting fluorescence intensity decay curves in terms of an exponential model, from which one or more fluorescence lifetime components are assigned based on an appropriate statistical fitting procedure. However, a problem arises when physical interpretation is sought for the apparent multiexponential intensity decay observed in proteins (or other macromolecular systems) containing a single fluorophore, or ostensibly, a single

Correspondence should be addressed to Enrico Gratton.

presumably homogeneous population of fluorophores. Such multiexponential decay is the rule rather than the exception in many proteins containing a single tryptophan residue (1). In principle, should a biexponential decay process be observed for a protein containing a single fluorophore, it seems quite reasonable to suggest the existence of two conformations of the protein. But it is usually difficult to rationalize the physical structure of the protein with the existence of two unique conformations even for the indole moiety only (8). Clearly, the inference regarding a number of unique conformations, in this instance two, is biased by the assignment of a biexponential decay. Furthermore, the limited resolvability of the data in lifetime components provided by current instrumentation (6, 7) does not allow one to distinguish among the different factors involved in the decay. The observed signal may easily constitute a superposition of heterogeneous decays comprising individual lifetime values that are very close to one another. The assignment of one or more exponentials to describe the overall decay process can hide the true physical origin of the lifetime heterogeneity (6, 7). Furthermore, given the sensitivity of the lifetime value to the different microenvironments and the multitude of different conformations present in a protein molecule (9, 10), there is no a priori reason to expect an exponential decay behavior for a residue in a protein except under very specific circumstances.

Here we present the analysis of fluorescence decay data obtained using multifrequency phase fluorometry of a few single tryptophan residue proteins in a limited temperature interval and in terms of distributions of lifetimes based, in good measure, on the principles outlined in the previous articles (7, 11). The fits obtained using a sum of exponentials, probability-density functions, and an analytical expression for the single-potential well lifetime distribution are compared and discussed. Preliminary accounts of the interpretation of the fluorescence lifetimes of the tryptophan moieties in proteins, and of the tryptophan itself in terms of distributions, have appeared previously (12, 13).

DISTRIBUTION OF LIFETIMES IN THE FREQUENCY DOMAIN

The derivation of the equations used for the fits reported here are briefly presented. Refer to the two previous papers (7, 11) for a complete discussion of the minimum resolvable width for a lifetime distribution of a given shape, for the ability to recover the distribution shape using probability density functions, and for the equations used to derive lifetime distributions using protein dynamics concepts.

The fluorescence intensity may be described by the following equation:

$$I_F(t) = \sum_{i=1}^{m} f_i \tau_i^{-1} e^{-t/\tau_i} \qquad i = 1 \ldots n, \tag{1}$$

where n is the total number of independent components of the decay. In Eq. 1, f_i is the fraction of light (photons) contributing to the total fluorescence by the ith component and the pre-exponential factor is proportional to the product $f_i\tau_i^{-1}$. In the limit when the number of components is large, Eq. 1 can be expressed in integral form:

$$I_F(t) = \int_0^\infty f(\tau)\tau^{-1}e^{-t/\tau}\,d\tau. \tag{2}$$

When a set of exponentially decaying components is excited by light intensity sinusoidally modulated at an angular frequency ω given by

$$E(t) = E_0\,[1 + M_e \sin \omega t], \tag{3}$$

where E_0 is the average intensity and M_e is the modulation of the excitation, respectively, the overall fluorescence response of the system can be written in the following form:

$$F(t) = F_0\,[1 + M_f \sin(\omega t - \phi)]. \tag{4}$$

F_0 and M_f are the average fluorescence and its modulation, respectively. The fluorescence is phase shifted with respect to the excitation by a value ϕ and demodulated such that the ratio $M = M_f/M_e < 1$. The measurable quantities at a given modulation frequency, ϕ and M, are related to the fluorescence decay in the time domain $I_F(t)$ by means of the following equations (14):

$$\tan \phi(\omega) = S(\omega)/G(\omega) \tag{5}$$

$$M(\omega) = [S^2(\omega) + G^2(\omega)]^{1/2}, \tag{6}$$

where

$$S(\omega) = 1/N \int_0^\infty I_F(t) \sin \omega t\,dt \tag{7}$$

$$G(\omega) = 1/N \int_0^\infty I_F(t) \cos \omega t\,dt \tag{8}$$

$$N = \int_0^\infty I_F(t)\,dt. \tag{9}$$

$I_F(t)$ contains the information of the distribution of components in the time domain. $S(\omega)$ and $G(\omega)$ are the sine and cosine Fourier transforms of $I_F(t)$ and N, a normalization factor.

The simplest approach to lifetime distributions assumes that the function $f(\tau)$ is of a given form; i.e., uniform, Gaussian, Lorentzian, and so on. The equations used for these unimodal and bimodal probability-density functions were given in reference 7. These functions (when normalized) are named probability density-functions due to the fact that data fits using this approach may recover the shape of the lifetime distribution within the limits of resolvability provided by the data in reference 7. A more general approach assumes that lifetime distributions for single tryptophan-residue proteins can be derived based on a physical model. For example, distributions of interconversion rates between two different environments (conformations), each with a characteristic quantum yield, will

yield distributions of lifetimes whose shape depends on the distribution of interconversion rates. This model is now under evaluation. Instead, the model used in this article has the analytical form for lifetime distribution derived for the single potential well (11) and it is briefly reported below. The basic assumption is that the probability of decay of an excited residue is determined by the radiative decay rate that is modulated by the environment. Consequently, an exponential decay is assigned to each environment, determined by the particular conformational coordinates of the residue and its local protein environment. The residue in its protein environment is then regarded as a semiclassic mechanical system. The potential energy is a function of the conformational coordinates and, depending on the particular protein, a single well or multiple-potential well may be considered. A potential well represents a stable conformation about which the conformational coordinates of the system oscillate (fluctuate). In the case of a single average conformation, the population of excited residues distribute in energy (dynamic plus conformational) following the Boltzmann distribution. In this model, the width of the well represents the degree of librational freedom of the fluorophore within its immediate environs in the protein, and is related to the density of energy states available in the potential well. In the case of excited tryptophan residues fluctuating around a set of conformational coordinates (11), the observed fluorescence decay is given by

$$I_F(t) = \int_0^\infty P(\epsilon)D(\epsilon)k_r e^{-k(\epsilon)t}d\epsilon, \quad (10)$$

where $P(\epsilon)$ represents the Boltzmann factor, ϵ is the energy, and T the temperature in energy units

$$P(\epsilon) = e^{-\epsilon/T}. \quad (11)$$

$D(\epsilon)$, the density of energy states in the particular well, has the following functional form:

$$D(\epsilon) = \text{const}'\,(\epsilon + \epsilon_0)^\beta \quad \beta < 0 \quad (12a)$$

$$D(\epsilon) = \text{const}\,(\epsilon - \epsilon_0)^\beta \quad \beta > 0. \quad (12b)$$

k_r is the radiative decay rate, assumed constant, and $k(\epsilon)$ is the average decay rate of the particular energy state. It is reasonable to assume that the higher the energy state, the more the residue experiences the different environments the faster is the average decay rate. The following functional form, which was justified in reference 11, was used for $k(\epsilon)$:

$$k(\epsilon) = A(T) + C(1 - e^{-\epsilon/T}). \quad (13)$$

When Eqs. 11–13 are used to conduct the integration of Eq. 10 in lifetime space, the following form was obtained:

$$I_F(t) = \int_{\tau_L}^{\tau_0} n(\tau)\tau^{-1}e^{-t/\tau}d\tau, \quad (14)$$

where

$$n(\tau) = N\tau^{-1}\{\ln[\tau(\tau_0 - \tau_L)/\tau_0(\tau - \tau_L)]\}^\beta \quad (15)$$

$$\tau_0 = A(T)^{-1} \quad (16)$$

$$\tau_L = [A(T) + C]^{-1}. \quad (17)$$

N is a normalization constant. Eq. 15 represents the lifetime distribution of each potential well and it was used to fit the fluorescence-decay data of the single tryptophan residue proteins presented here. To account for the heterogeneity of each energy state, Eq. 15 was convoluted with a Gaussian of width indistinguishable from a single exponential (7). In particular, Eq. 15 was substituted in Eq. 14 and then the functions $S(\omega)$ and $G(\omega)$ were calculated using Eqs. 7 and 8. The values of phase and modulation can be determined using Eqs. 5 and 6. Other functional forms for $n(\tau)$ corresponding to different probability density functions (7) were also used.

METHODOLOGY

The fluorescence decay was measured by use of multifrequency phase fluorometry (15) on an instrument that utilizes the harmonic content of a mode-locked, synchronously pumped and frequency-doubled dye laser as an excitation source. The operational principles of this instrument and some applications to protein studies have been reported (16). This instrument provides a resolution of ~0.1% in phase and modulation values and tunable ultraviolet excitation in the 280–310-nm range, with a linewidth of ~0.06 nm. In the reference cell a solution of p-terphenyl in cyclohexane was used to correct for possible "color errors" (17). A lifetime of 0.99 ns was assigned to this reference. An excitation polarizer at 55° with respect to the horizontal eliminated possible polarization effects. The emission was observed using two LG-350 filters to eliminate scattered radiation from the laser. The modulation frequencies employed were in the 1–400-MHz range. Generally, 8 to 16 different modulation frequencies were used for each data set. Data were collected until the standard deviation from each measurement of phase and modulation were at the most 0.2° and 0.004, respectively. The measurements on each individual protein were repeated at least three times using independent preparations.

The wavelength used here to excite the protein was 300 nm, which corresponds to the red edge of the absorption of tryptophan. At this wavelength tyrosine residues are not excited, which minimizes heterogeneity of the emission due to excitation of more than one species and also minimizes energy transfer from tyrosine to tryptophan residues. Additionally, 300 nm excitation selects a population of tryptophan residues not likely to be affected by dipolar relaxation processes occurring during the excited-state lifetime. This excitation wavelength does not eliminate the risk of tyrosinate excitation and emission, but any possible effects of the latter are mitigated by the low quantum yield of tyrosinate emission (18, 19) and also its apparently rare occurrence in proteins. Further, from their spectral characteristics, there is no reason to suspect the contribution of tyrosinate fluorescence in any of the proteins studied. These were all necessary conditions to be considered before further evaluation of the data, irrespective of the analytic method employed.

The sample temperature was controlled using an external bath circulator (model LT50; Neslab Instruments Inc., Portsmouth, NH). The temperature of the sample was measured before and after each measurement in the sample cuvette using a digital thermometer (model 410B-TC; Omega Optical Inc., Brattleboro, VT). Solutions were not deoxygenated.

For the data fits a nonlinear least-squares algorithm for the multiexponential analysis (20) and a Simplex algorithm (21) for the distributional analysis were used. In both cases, the function to be minimized was the reduced χ^2 defined by

$$\chi^2 = \Sigma_j\{[(\phi_j^c - \phi_j^m)/\sigma_j^\phi]^2 + [(M_j^c - M_j^m)/\sigma_j^M]^2\}/(2n - f - 1), \quad (18)$$

where ϕ_j^c and M_j^c are the calculated values of phase and modulation, respectively, according to Eqs. 5 and 6; ϕ_j^m and M_j^m are the measured values of phase and modulation at the frequency ω; σ_j^ϕ and σ_j^M are the standard deviations of the measurements of phase and modulation, respectively; f is the number of degrees of freedom and n the number of modulation frequencies. An acceptable fit should give a value of χ^2 close to unity. However, to expedite calculations, the value of σ_j^ϕ and σ_j^M were assumed to be the same for each measurement j, so that the common value of the standard deviation can factorize out from Eq. 18. A value of 0.2° and 0.004 was used for the standard deviation of phase and modulation determination, respectively. These values were very close to the experimental standard deviations, since data were acquired at each modulation frequency until the desired standard deviation was reached. The values of the parameters obtained in the fit are independent of the common value assumed for the standard deviations (20). Using this procedure, the values of the χ^2 can be different from one even for a good fit. However, here we compare the values of the χ^2 obtained using different models but using the same values for the standard deviation. We should note that phase modulation fluorometry offers the equivalent of delta function excitation (zero-pulse width) in the time domain. This means that problems inherent in deconvolution of measured intensity decay profiles are avoided; when such problems exist, they can complicate the analysis of $I_F(t)$ curves in terms of distributions of lifetimes.

Each enzyme preparation (determined by lot number) was subject initially to SDS-polyacrylamide gel electrophoresis and assayed for activity by published methods (22). Ribonuclease T1 (RNAse T1) was obtained from Boehringer-Mannheim. The protein was >98% pure by electrophoretic analysis and had high specific activity. RNAse T1 was prepared for study by dialysis vs. 0.025 M MOPS, 0.125 M KCl, pH 7.0 (1 liter × 2 changes). An extinction coefficient of 19 ($\epsilon_{1\%,1\,cm}$) was used to determine the concentration of RNAse T1. Scorpion neurotoxin variant 3 (NTV3) and variant 2 (NTV2) were the kind gift of Dr. D. D. Watt (Univeristy of Nebraska) and were >98% pure by SDS-gel and HPLC analysis. Phospholipase A2 (PLA2) and prophospholipase A2 (proPLA2) were purified from porcine pancreas and were the gift of Dr. H. S. Hendrikson (St. Olaf College, Northfield, MN). This enzyme was assayed for activity by use of a novel fluorescence assay using a naphthyl-vinyl glycerophosphocholine analogue developed by Dr. H. S. Hendrickson. The assay showed the PLA2 preparation used to be of the highest specific activity obtainable (H. S. Hendrickson, personal communication). These proteins were judged to be pure by electrophoretic criteria. X-ray crystallographic data were obtained from the Brookhaven Protein Data Bank (23) except for the depiction of RNAse T1 that were obtained from x-ray coordinates. Molecular graphics depictions were prepared from the x-ray derived coordinates by use of the program HYDRA (24) implemented on the VAX 11/750 and displayed on an Evans & Sutherland PS 330 picture system (Salt Lake City, UT).

RESULTS

Although the data described below relate exclusively to fluorescence lifetimes, it is worthwhile to mention briefly a few details regarding other optical spectral properties of the proteins. The fluorescence emission spectra of RNAse T1, PLA2, and NTV3 show maxima at 320, 334, and 339 nm, respectively, when excited at 300 nm, the excitation wavelength used for lifetime measurements in our experiments. In all proteins, excitation at 280 nm resulted in an increase in quantum yield of apparent tryptophan emission in excess of that expected by an increased extinction coefficient. This was particularly noticeable in RNAse T1 and is most likely due to energy transfer from tyrosyl residues as noted by Oobatake et al. (25). Avoidance of energy transfer is obviously paramount for fluorescence lifetime studies. Using excitation at 300 nm there was no anomalous "lengthening" of the lifetime determined from the phase angles, which, if it had been present, would have signified existence of energy transfer (26). Lastly, absorption and emission spectra showed no unusual features to suggest interference from any extraneous substances.

In Table I we present the phase and modulation data obtained for tryptophan in water at pH 6, tryptophan in glycerol, *n*-acetyl-tryptophan amide (NATA), 5-methyl indole in $CH_{3\alpha}CN$ and in α-cyclodextran. We present also data obtained at 25°C for the five single tryptophan proteins investigated here. The major criteria for inclusion in the study were that each protein should have a single tryptophan residue, that the protein should be monomeric and that the crystal structure of each should be available. The first-mentioned criterion assures the simplest possible protein system for study, while the last-mentioned criterion should allow eventually a correlation to be drawn between the protein's structure and its luminescence characteristics. Phase and modulation data were collected at least three times for each protein preparation. Different runs gave identical results. This section presents the results of the fits using different functions to describe the decays. First, the fluorescence decay is analyzed using sum of exponentials, Secondly, probability-density functions of different shape were used with the intent of recovering the shape of the lifetime distribution (7). Of course, this approach gives no direct insight on the physical origin of the distribution. Finally, the function for lifetime distributions derived in our previous paper (11) based on the description of the single-potential well with multiple-energy substates was employed for the fits.

Exponential Fits

In Table II we present the values of the components lifetime, fractional intensities, and χ^2 for the tryptophan preparations and derivatives and for the proteins investigated. For the tryptophan derivatives, a single exponential decay satisfactorily described the decay. For all of the proteins studied, the fit to the data required the use of at least two, and in two instances (PLA2 and proPLA2) three decaying components. Such apparent multiexponentiality in the decay has been observed before in these and other proteins containing single fluorophores (1). Indeed, the lifetime values of PLA2 and proPLA2 that we report from the three component analysis from the fluorescence of porcine pancreatic PLA2 agree well with those reported recently by Ludescher et al. (27) from a time-correlated photon-counting experiment on the same system. The apparent multiexponentiality of the intensity decays in these systems has led to the inferences that there are several conformers of a protein (27) each giving rise to a unique lifetime. Given the data, such inferences are inherently reasonable, but there is no intrinsic reason why the "individual" lifetime values cannot represent the statistical

TABLE 1
PHASE DELAY AND MODULATION RATIO MEASUREMENTS AT 25°C

	Frequency	Phase	Modulation
	MHz	*degrees*	
Tryptophan pH 6	7.2	7.78	0.987
	19.2	20.32	0.926
	43.2	39.40	0.753
	86.3	56.69	0.517
	138.9	69.28	0.353
	158.1	72.12	0.321
	297.1	81.79	0.189
Tryptophan in glycerol	5.10	10.17	0.983
	10.44	19.99	0.868
	20.44	35.00	0.810
	30.44	45.56	0.688
	40.88	53.52	0.580
	81.82	69.82	0.343
	112.26	75.75	0.257
	142.70	79.02	0.204
	194.08	82.30	0.152
NATA	1.04	1.74	0.999
	3.06	5.63	0.996
	5.70	10.15	0.985
	11.06	19.02	0.948
	21.71	33.36	0.839
	30.39	43.46	0.739
	51.06	56.08	0.550
	63.86	63.66	0.457
	81.87	67.63	0.373
	112.26	75.33	0.283
	142.65	79.03	0.224
	176.12	82.15	0.191
	224.52	84.28	0.144
5 Methylindole in CH_3CN	5.61	10.54	0.984
	7.86	14.33	0.971
	10.10	18.27	0.952
	13.47	23.99	0.917
	16.84	29.13	0.879
	18.71	31.96	0.850
	37.41	50.87	0.628
	56.12	61.54	0.463
	74.83	67.15	0.374
	93.53	73.08	0.327
	112.24	75.24	0.258
	130.95	79.43	0.230
5-Methyl indole in α-cyclodextran	23.16	56.94	0.532
	57.16	74.17	0.252
	81.82	78.20	0.177
	138.97	82.40	0.107
	196.13	82.93	0.053
	277.95	83.20	0.053
PLA2 in buffer with Ca^{++}	21.10	21.48	0.885
	30.44	27.64	0.814
	40.44	33.33	0.741
	81.81	45.92	0.543
	112.24	51.83	0.452
	142.68	55.35	0.387
	194.05	60.02	0.317
	224.49	62.43	0.286

TABLE 1
(*Continued*)

	Frequency	Phase	Modulation
ProPLA2 in MPOS, KCl	5.10	9.22	0.983
	10.44	17.70	0.929
	20.44	29.72	0.809
	30.44	37.71	0.699
	40.88	43.22	0.605
	81.82	54.59	0.404
	112.26	59.10	0.330
	142.70	62.09	0.277
	194.08	65.99	0.222
	224.52	68.27	0.200
	336.78	72.81	0.141
RNAse T1 in buffer	21.10	24.13	0.906
	30.44	32.59	0.829
	40.44	39.64	0.747
	81.81	57.21	0.505
	112.24	63.63	0.393
	142.68	67.59	0.322
	194.05	71.52	0.246
	224.49	75.99	0.206
NTV3 in buffer	21.10	5.27	0.965
	30.44	6.81	0.968
	40.44	8.25	0.955
	81.81	14.37	0.915
	112.24	18.26	0.887
	142.68	22.15	0.855
	194.05	27.88	0.822
	224.49	32.30	0.789
	336.73	42.39	0.670

averages of several fluorescence lifetimes, rather than unique values related to unique conformations of the proteins.

Probability Density Functions

Below we analyze and discuss fluorescence decay data of the above proteins based on a variety of probability-density functions from which general trends of the behavior of the lifetime distribution with temperature can be obtained.

Unimodal Probability Density Function Fits. The three two-parameter functions used were the uniform, the Gaussian, and the Lorentzian (Table III). The two parameters that define each probability-density function are the center and the width (7). The three functions are symmetric about the center that corresponds to the average value of the distribution. For the three functions the widths are defined as the full-width-half-maximum (FWHM). All distributions used here were normalized and defined only in the positive lifetime domain. Fig. 1 shows the center and the width values obtained for the fits using the uniform probability density function to the PLA2 data for the temperature range from 4.9° to 33.3°C. The following trends can be observed: (*a*) the distribution (its center) shifts to lower lifetime values

TABLE II
DISCRETE COMPONENT ANALYSIS OF DATA IN TABLE I

	τ_1	f_1	τ_2	f_2	τ_3	f_3	χ^2
	ns		*ns*		*ns*		
Tryptophan in aqueous solution pH 6							
1	3.03 ± 0.04	1.00					1.5
2	2.91 ± 0.15	0.95 ± 0.10	8.48 ± 9.96	0.05			1.4
Tryptophan in glycerol							
1	5.43 ± 0.07	1.00					3.0
2	5.50 ± 0.10	0.96 ± 0.02	37.6 ± 37.2	0.04			2.2
NATA							
1	4.81 ± 0.03	1.00					1.2
2	4.95 ± 1.94	1.11 ± 0.12	6.36 ± 25.85	−0.11			1.2
5-Methylindole in CH_3CN							
1	5.25 ± 0.04	1.00					2.4
2	5.44 ± 2.36	1.16 ± 4.53	6.82 ± 22.49	−0.16			2.4
5-Methylindole in α-cyclodextran							
1	10.76 ± 0.32	1.00					2.5
2	10.71 ± 0.53	1.00	0.02	0.00			2.4
PLA2 in buffer with Ca^{++}							
1	2.18 ± 0.17	1.00					841
2	4.02 ± 0.11	0.72 ± 0.02	0.87 ± 0.04	0.28			7.1
3	5.39 ± 0.36	0.42 ± 0.06	2.16 ± 0.27	0.43 ± 0.04	0.60 ± 0.06	0.15	0.7
PropPLA2 in MOPS, KCl							
1	3.38 ± 0.22	1.00					985
2	5.67 ± 0.11	0.81 ± 0.01	0.99 ± 0.04	0.19			8.8
3	6.62 ± 0.12	0.66 ± 0.02	2.29 ± 0.18	0.25 ± 0.02	0.66 ± 0.04	0.09	0.7
RNAse T1 in buffer							
1	3.13 ± 0.08	1.00					79
2	3.61 ± 0.05	0.92 ± 0.02	1.07 ± 0.12	0.08			2.7
NTV3 in buffer							
1	0.47 ± 0.02	1.00					104
2	4.36 ± 0.51	0.09 ± 0.01	0.42 ± 0.01	0.91			3.2

monotonically as the temperature increases. The higher the temperature, the shorter the average lifetime. (*b*) The distribution becomes narrower with increasing temperature. The same qualitative behavior was observed using the Gaussian and Lorentzian functions (data not shown). Furthermore, the same results were obtained in the cases of NTV3 and RNAse T1, irrespective of the probability density function used. We previously reported similar results (12, 13). With exception of the Gaussian fit to PLA2 in the temperature range from 20° to 25°C, the three symmetric unimodal probability-density functions mentioned here do not fit the data as judged from the χ^2 value (Table III). We note that in this case we have only two independent parameters in the fit, the center and the width (FWHM).

Bimodal Probability Density Functions. Bimodal uniform, Gaussian, and Lorentzian probability-density functions were also used to fit the fluorescence decay data from NTV3, PLA2, and RNAse T1 (Table III). Fig. 2 shows the results obtained for the bimodal uniform distribution. The shapes of the distribution obtained are clearly asymmetric. Furthermore, the two trends observed above using the unimodal probability density functions were also present in this case (data not shown): The center of gravity of all bimodal probability-density functions monotonically shifted to lower lifetime values and the overall distribution became narrower as the temperature was increased. It should be mentioned that the data fits using bimodal probability-density functions required five parameters (two centers, two widths, and the relative ratio of the two components of the distribution).

Single-Potential Well Fits

Fig. 2 (shaded areas) shows the single-potential well lifetime distribution of PLA2, RNAse T1 and NTV-3 at 25° C. Table IV reports the parameters obtained using this

TABLE III
PARAMETER FITS OF PROBABILITY DENSITY FUNCTIONS AT 25°C

Function	F1	C1	W1	C2	W2	χ^2
PLA2 (unimodal)						
Lorentzian	1.00	2.40	2.79			10.65
Gaussian	1.00	2.50	5.98			0.77
Uniform	1.00	3.21	5.92			1.45
PLA2 (bimodal)						
Lorentzian	0.47	1.37	1.21	4.33	0.38	0.79
Gaussian	0.81	3.01	4.93	5.91	2.94	0.75
Uniform	0.93	3.32	5.20	6.20	3.35	0.70
RNAse-T1 (unimodal)						
Lorentzian	1.00	3.31	0.78			6.64
Gaussian	1.00	3.52	2.69			5.31
Uniform	1.00	3.55	4.29			10.84
RNAse-T1 (bimodal)						
Lorentzian	0.93	3.60	0.05	1.07	0.02	2.79
Gaussian	0.83	3.67	0.55	1.34	0.90	2.94
Uniform	0.92	3.62	0.65	1.07	0.33	2.71
NTV-3 (unimodal)						
Lorentzian	1.00	0.44	0.28			16.47
Gaussian	1.00	0.49	0.70			37.27
Uniform	1.00	0.52	0.85			38.78
NTV-3 (bimodal)						
Lorentzian	0.92	0.43	0.05	4.69	2.46	2.59
Gaussian	0.89	0.43	0.25	5.01	7.32	3.18
Uniform	0.91	0.43	0.24	4.84	7.62	2.86

C = center (in nanoseconds). W = full width at half maximum (in nanoseconds). F = fraction.

model. Measurement on NTV-2, which is similar to NTV-3 in amino-acid sequence (27a) and in x-ray structure (27a, 28) show that the form of the distribution is essentially identical, with perhaps a slight preponderance of longer-lived components. Small changes of the shape of the distribution of RNAse T1, NTV-2, and NTV-3 in the temperature range studied (4.9°–33.3°C) were observed (data not shown) to follow the two trends discussed above. Fig. 3 shows the single-potential well fits for PLA2 in the temperature range from 4.9° to 33°C. Again, the distribution center of gravity shifted toward longer lifetime values

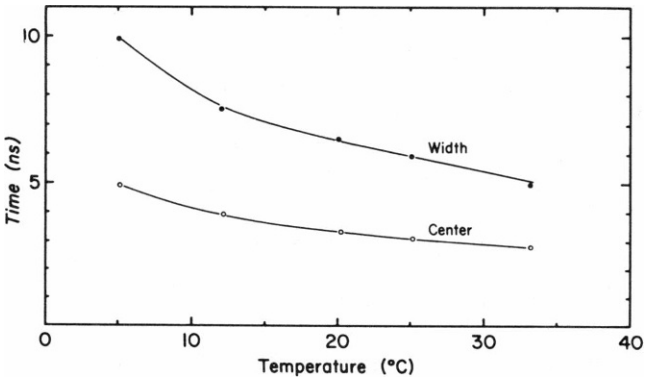

FIGURE 1 Center and width values as a function of temperature obtained from the analysis of PLA2 data using the unimodal uniform probability-density function.

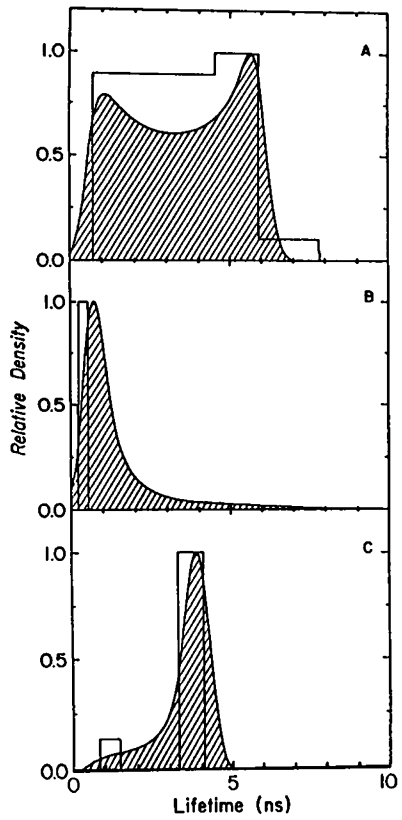

FIGURE 2 Comparison between overlapping bimodal uniform probability-density functions (*light curves*) and the lifetime distribution (*shaded curves*) of the single-potential well model using data at 25°C. Both approaches recover the shape of the distribution. At higher temperatures the agreement becomes even better. (*A*) PLA2, (*B*) NTV3, and (*C*) RNAse T1.

and the average width became larger as the temperature was decreased. The lifetime distribution of proPLA2 (not shown) followed the same trend.

From Tables II and IV we can compare the χ^2 values of the two-exponential components analysis and of the single-potential well analysis. Both fits involve the use of three fitting parameters. The discrete component analysis includes two lifetimes and one fraction. The single-potential well analysis includes the maximum and mini-

TABLE IV
SINGLE POTENTIAL WELL ANALYSES

A. Parameter fits of single-potential well distribution at 25°C

	$\tau_L(ns)$	$\tau_0(ns)$	β	χ^2
PLA2	0.31	6.05	−0.44	2.09
RNAse-T1	0.31	3.98	−1.49	2.94
NTV-3	0.25	19.14	−0.34	3.03

B. Single-potential well parameter fits of PLA2

T (°C)	$\tau_L(ns)$	$\tau_0(ns)$	β	χ^2
4.9	0.29	7.21	−0.74	13.03
12.0	0.34	7.08	−0.51	5.10
20.5	0.33	6.61	−0.45	3.23
25.4	0.31	6.05	−0.43	2.09
33.3	0.35	5.76	−0.34	1.16

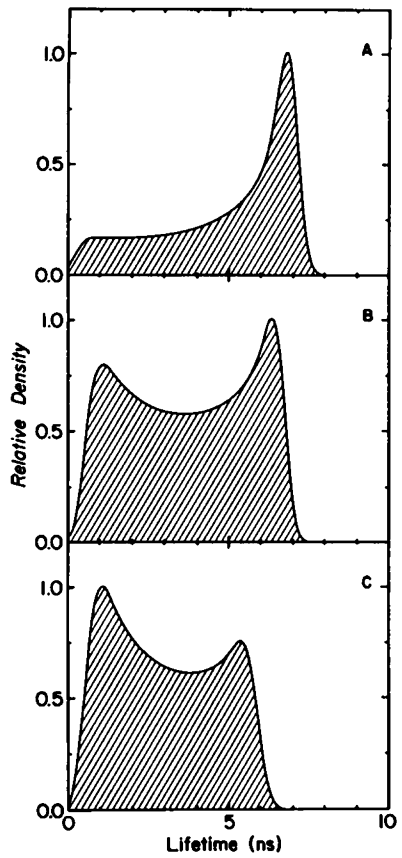

FIGURE 3 Evolution of the lifetime distribution of PLA2 with temperature. As the temperature increases the center-of-gravity shifts to shorter lifetimes and the distribution becomes narrower. *A*, *B*, and *C* correspond to data fits at 4.9°, 20.5°, and 33.3° C, respectively.

mum lifetime limits over which the distribution extends, and the power law of the density of states that is a measure of the potential well width, or equivalently, a measure of the motional degree of freedom allowed by the conformation. In the case of PLA2, the two-component model does not fit the data, but the single potential well distribution does fit all three proteins with comparable or smaller χ^2 values than were obtained for the two component model. For the single-potential well distribution of this protein, the value of the exponent of the function density of states decreased at lower temperature, which can be interpreted as a restriction of the motional freedom at lower temperature (11). However the χ^2 value of the single-potential well fit was higher at lower temperature (Table IV) indicating a progressive failure of the model at lower temperatures.

DISCUSSION

The Meaning of Lifetime Distributions

The interpretation of the fluorescence decay for a series of four proteins and at several temperatures using lifetime distributions assumes that lifetime heterogeneity arises from a multitude of different conformations. One must distinguish between the actual value of the average fluorescence lifetime and the distribution of lifetimes about that average value. Neither from this data nor from the distribution analysis presented above can we speak sensibly to the issue of the factors determining the actual value of the lifetime. These factors will almost certainly be dictated by the influence of the environs on the excited state of the fluorophore, while the distribution per se is, in our view, dominated by the peculiarities of the potential well in which the aromatic side-chain librates. The distributional approach we present is dominated by the assumption that the mobility of the residue is the major determinant of the form of the distribution, but may be less important as a determinant of the lifetime value per se. The motion of the indole ring, determined by rotations about the χ_1 and χ_2 dihedral angles, will allow the fluorophore to sample the entire microenvironment of the potential well in which it is rotating or librating. This in turn means that the fluorophore will be influenced variably by the moieties local to a particular region of the potential well. The shape of the distribution, therefore, will depend on the free volume available for motion. A broad distribution would be expected for tryptophan residues free to move through large angles. Such a situation is more likely for residues on the surface of proteins or in water-filled pockets, given the obvious constraints put on the existence of empty volumes in the interior of proteins. The tryptophan in PLA2 provides an excellent case in point as it lies on the surface of the protein fully exposed to solvent. The molecular graphics display shown in Fig. 4 makes the motional freedom of the residue quite apparent. The same conclusion has been drawn by other authors, most recently by Ludescher et al. (27), who have also suggested the existence of a distribution of states to explain the apparent multiexponentiality of the fluorescence decay in PLA2. This inference is also supported by the relatively low, steady state anisotropy values noted for tryptophan fluorescence of PLA2 (27). It is important to note that torsional motions of the indole ring per se might contribute to the occupation of different states. Howard and Schalg (29) have provided evidence that in a low-pressure gas there is a dependence of the fluorescence emission on rotational motions, and that this influence is extended to both radiative and nonradiative rates. Similarly, Engh et al. (30) and James and Ware (31) have argued that the nonexponentiality of the fluorescence of free tryptophan is due to the existence of a distribution of states. In the models of these authors potential barriers to torsional motions about the χ_1 and χ_2 and dihedral angles cause librations within geometrically defined potential wells. The extent of interaction with local moieties capable of affecting the fluorescence properties of the indole, varies with the well and, consequently, so does the fluorescence lifetime. The experimental evidence for the existence of such multiple rotamers in free tryptophan is good (32–34) and the mechanisms of fluorescence quenching proposed by Engh et al. is reasonable (30). A similar

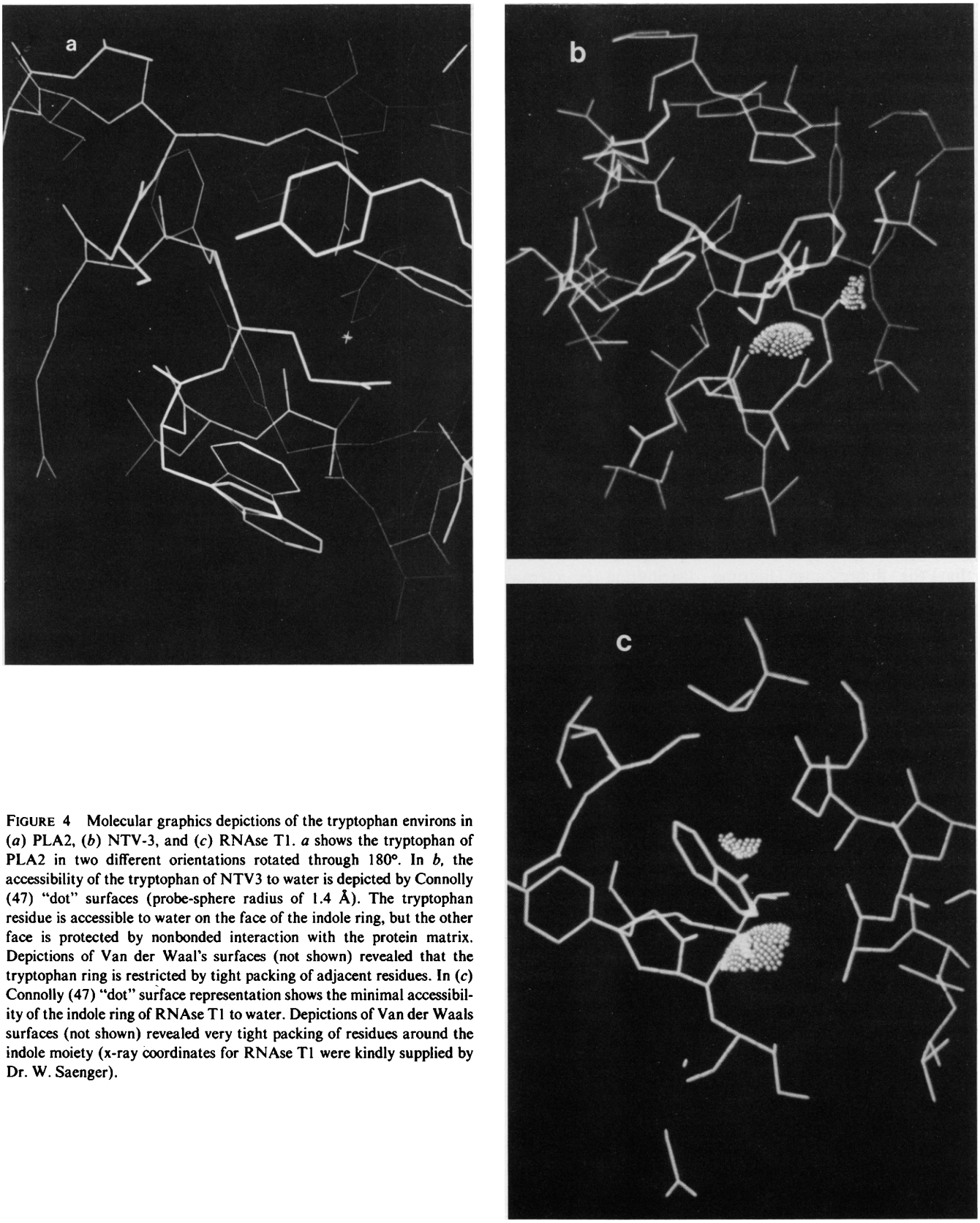

FIGURE 4 Molecular graphics depictions of the tryptophan environs in (*a*) PLA2, (*b*) NTV-3, and (*c*) RNAse T1. *a* shows the tryptophan of PLA2 in two different orientations rotated through 180°. In *b*, the accessibility of the tryptophan of NTV3 to water is depicted by Connolly (47) "dot" surfaces (probe-sphere radius of 1.4 Å). The tryptophan residue is accessible to water on the face of the indole ring, but the other face is protected by nonbonded interaction with the protein matrix. Depictions of Van der Waal's surfaces (not shown) revealed that the tryptophan ring is restricted by tight packing of adjacent residues. In (*c*) Connolly (47) "dot" surface representation shows the minimal accessibility of the indole ring of RNAse T1 to water. Depictions of Van der Waals surfaces (not shown) revealed very tight packing of residues around the indole moiety (x-ray coordinates for RNAse T1 were kindly supplied by Dr. W. Saenger).

inference may be drawn for tyrosine fluorescence from the recent data of Ross and co-workers (35, 36).

Despite what we have stated above, the mere fact that a tryptophan is fully exposed to solvent does not inevitably mean a high degree of mobility. For example, some tryptophan residues show strong nonbonded interactions with the protein matrix such that they appear to lie on the surface of the protein, whereupon motion about the $C\alpha$-$C\beta$ and $C\beta$-$C\gamma$ bonds must be minimal (37). Good examples of this situation are found in W15 of the liver alcohol dehydrogenase and W48 of staphylococcus nuclease (37). The tryptophan of NTV3 (Fig 4) appears to be similarly disposed though not quite as stringently as, say, W15 of LADH. The environment of the tryptophan in NTV3 is however, made rather unusual by the close proximity of a cluster of tyrosyl residues. At least one of these must be interacting strongly with the tryptophan ring given the clear evidence of ring current effects on the proton NMR resonances of the indole moiety in this protein (28). Thus, the tryptophan in NTV3 also suffers a number of likely restrictions on its motion, and these are probably the determinants of the relatively narrow distribution of lifetimes, the short average fluorescence lifetimes being determined by the electronic character of the fluorophore's environs. Our approach would suggest that the mobility of the tryptophan in RNAse T1 is also highly restricted so that the fluorescence lifetime distribution is narrow. Indeed James et al. (38) have suggested that the tryptophan fluorescence intensity decay in RNAse T1 is monoexponential.

So far, we have used water accessibility implicitly as an indicator of the likely free volume available for the tryptophan residue to move. The graphics depiction of Fig. 4 shows clearly that water has very limited access to the indole moiety in RNAse T1 (39), which support the conjectures of Eftink and co-workers (40, 41) and James et al. (38), who inferred such limited accessibility on the basis of fluorescence-quenching data. Calculation of the average distances of separation by use of van der Waals surfaces show the "pocket" in which the tryptophan is very tightly packed (Fig. 4). These inferences based on the graphics data and the fluorescence-quenching results are also supported by steady state and time-resolved anisotropy data (41), which suggest that the indole ring in RNAse T1 is essentially incapable of much local motion.

Temperature Effects

The previous paper (11) shows that the dynamic nature of the protein can affect the fluorescence decay. We reasoned that in the limiting case of the frozen protein (negligible dynamics), one may consider that the fluorescence is determined by a set of exponentials for which the lifetimes and amplitudes are characteristic of the set of environments of the excited residues in the protein. However, as the dynamic nature of the protein is allowed to play its role, the excited tryptophan residues become exposed to electronic environments, the nature of which vary with time. Then the set of amplitudes and decay times that characterizes the overall fluorescence will no longer resemble the set of static environments to which the excited residues are exposed in the frozen protein. The two general trends of the characteristic parameters of the lifetime distribution observed as the temperature was changed for the proteins studied with their single tryptophan residues exposed to quite different environments can be qualitatively explained as follows. As the temperature increases, the rate at which the protein fluctuates in stable conformations and the rates at which it interconverts among different conformations increases. The localized environment in the protein matrix experienced by the tryptophan residue during its excited lifetime becomes more homogeneous, which leads to a more homogeneous decay and the resulting narrow distribution. Broad distributions as those seen in PLA2 should therefore narrow substantially at higher temperature. This model suggests (and our data support the view) that intrinsically narrow distributions are not likely to be markedly influenced in width by increasing the temperature. In the case of NTV3 and RNAse T1 the shape (as obtained from the probability density functions fit and as measured by the value of the exponent β) of the lifetime distribution as a function of temperature remains relatively narrow at low temperature, suggesting that the tryptophan residues in these proteins have restricted mobility around an average conformation.

The single-potential well model used to derive continuous lifetime distributions seems to have limited applicability for PLA2. The temperature behavior of the lifetime distribution for this protein (Table IV) shows that the fit becomes poorer at lower temperature. However, the values of the exponent β of the density of states function decreased at lower temperature, corresponding to a restricted mobility of the tryptophan residue at lower temperature, as should be expected. Instead, the value of τ_0 became larger at lower temperature, indicating a wider distribution of conformational substates (11), which can be considered as an evidence for the existence of a multiple-potential well for this protein. The broadening of the lifetime distribution at lower temperature seems to be present in all proteins investigated, although with less emphasis for RNAse T1 and NTV3, suggesting that the multitude of conformational substates proposed for proteins (9–10) can be responsible for this behavior.

Example of Single-Exponential Decay

Finally we mention the fluorescence analysis of tryptophan, tryptophan derivatives, and 5-methyl-indole sequestered in a pocket formed by α-cyclodextrin. This complex in aqueous environments displays a structured fluorescence-emission spectrum maximum at 308 nm and other spectral properties suggesting complete protection from solvent accessibility (42; F. G. Prendergast and E. Gratton, unpublished observations). Analysis of the decay using

exponentials yielded a fluorescence lifetime of 10.7 ns. The distribution analysis for these indole derivatives collapsed to a single exponential, or more precisely, if the resolvability provided by the data (0.1% error in the measurable quantities) is taken into account, the fluorescence decay can be described by any distribution function of width indistinguishable from a single exponential.

CONCLUSIONS

The fluorescence lifetime distribution is determined by the multitude of conformational substates in a protein and by the dynamics of the protein as experienced by the tryptophan residue. Such a statement is supported by fits to fluorescence-decay data using probability-density functions and by the single-potential well model. The range of conformational substates differing in lifetime value changes markedly from one protein to another. The results show that the average lifetime of the decay and the width of the distribution decrease their value with increasing temperature. Such behavior is characteristic of the model analyzed in the previous paper (11). Fits to data from the four proteins studied here, in aqueous solutions, in the limited temperature range and with very different environment for the single-tryptophan residues show that at temperatures higher than 25°C, the tryptophan residues fluctuate among different substates at rates comparable or higher than their excited state fluorescence lifetimes in the respective proteins. The suggestion that there are conformational substates in proteins is obviously not new (9, 10), and the fluorescence method we describe may provide a good approach to the study of conformational substates and of the energetics of such substates providing further validation of the distributional model. One particular advantage of the fluorescence approach can be the apparent ability to quantify the interconversion rates and therefore, to be able to approach or access the time scale of the events predicted by the molecular dynamics calculations (5, 43). Further development of the distribution model will require correlation of its predictions with the structure of the proteins under study and with the results of molecular dynamics calculations. The sensitivity of the apparent structural fluctuations to temperature and to ligand binding and sites on the protein remote from the fluorophore's location, and the role of preferential (but noncovalent) interactions of the fluorophore with the protein matrix in determining the form of the distribution, all need to be examined. In addition, more detailed studies using molecular dynamics simulations must be done to characterize the dynamics of the indole ring in proteins. The value of determining the two-dimensional potential energy surface of the indole ring about the χ_1 and χ_2 dihedral angles have been amply demonstrated by the recent work of Haydock and Prendergast (44) and Engh et al. (30). Also a more complete understanding of the role of electrostatic interactions in determining the actual (average) value of the fluorescence lifetime of indole moieties is essential. Preliminary data relating to this question have recently appeared (45, 46).

The results presented here were obtained from preliminary and incomplete data, i.e., no studies of the quantum yield as a function of temperature were presented that are suggested by our model (11). Collection of data over a wider temperature range and fits using the interconverting conformational model (two-potential well) is in progress. The analysis we have provided represents only an initial attempt to interpret the nature of tryptophan-fluorescence lifetimes in proteins.

We would like to acknowledge Mr. Peter Callahan for his help in the collection of data and in the preparation of the figures of this manuscript and Dr. J. P. Palmeri for helping with the data fitting.

This work was possible thanks to the financial support to Enrico Gratton from the National Science Foundation grant PCM 84-03107 and a Naval Research Grant MDA 903-85-X-0027, and to Franklin G. Prendergast from GM 34847. Franklin G. Prendergast was an Established Investigator of the American Heart Association during the performance of this project.

Received for publication 3 October 1986 and in final form 10 February 1987.

REFERENCES

1. Beechem, J. M., and L. Brand. 1985. Time resolved fluorescence decay in proteins. *Annu. Rev. Biochem.* 54:43–71.
2. Lakowicz, J. R., and G. Weber. 1973. Quenching of protein fluorescence by oxygen. Detection of structural fluctuations in proteins on the nanosecond time scale. *Biochemistry.* 12:4171–4179.
3. Careri, G., P. Fasella, and E. Gratton. 1979. Enzyme dynamics: the statistical physics approach. *Annu. Rev. Biophys. Bioeng.* 8:69–97.
4. Careri, G., P. Fasella, and E. Gratton. 1975. Statistical time events in enzymes: a physical assessment. *CRC Crit. Rev. Biochem.* 3:141–164.
5. Karplus, M., and J. A. McCammon. 1983. Dynamics of proteins, elements and function. *Annu. Rev. Biochem.* 53:263–300.
6. James, D. R., and W. R. Ware. 1985. A fallacy in the interpretation of fluorescence decay parameters. *Chem. Phys. Lett.* 120:455–459.
7. Alcala, J. R., E. Gratton, and F. G. Prendergast. 1987. Resolvability of fluorescence lifetime distributions using phase fluorometry. *Biophys. J.* 51:587–596.
8. Szabo, A. G., T. M. Stepanik, D. M. Wayner, and N. M. Young. 1983. Conformational heterogeneity of the cooper binding site in azurin. *Biophys. J.* 41:233–244.
9. Austin, R. H., K. W. Beeson, L. Eisenstein, H. Frauenfelder, and I. C. Gunsalus. 1975. Dynamics of ligand binding to myoglobin. *Biochemistry.* 14:5355–5373.
10. Ansari, A., J. Berendzen, S. F. Bowne, H. Frauenfelder, I. E. T. Iben, T. B. Sauke, E. Shyamsunder, and R. D. Young. 1985. Protein states and proteinquakes. *Proc. Natl. Acad. Sci. USA.* 82:5000–5004.
11. Alcala, J. R., E. Gratton, and F. G. Prendergast. 1987. Fluorescence lifetime distributions in proteins. *Biophys. J.* 51:597–604.
12. Gratton, E., J. R. Alcala, G. Marriott, and F. G. Prendergast. 1986. Fluorescence studies of protein dynamics. Proc. Internat. Symp. Computer Analysis for Life Science, Hayashibara Forum '85, Okayama, Japan. C. Kawabata and A. R. Bishop, editors. 1–11.
13. Alcala, J. R., G. Marriott, E. Gratton, and F. G. Prendergast. 1986. Fluorescence lifetime distributions in single tryptophan proteins. *Biophys. J.* 49(2, Pt. 2):108a. (Abstr.)

14. Weber, G. 1981. Resolution of the fluorescence lifetimes in a heterogeneous system by phase and modulation measurements. *J. Phys. Chem.* 85:949–953
15. Gratton, E., and M. Limkeman. 1984. A continuously variable frequency cross-correlation phase fluorometer with picosecond resolution. *Biophys. J.* 44:315–324.
16. Alcala, J. R., E. Gratton, and D. M. Jameson. 1985. A multifrequency phase fluorometer using the harmonic content of a mode-locked laser. *Anal. Instrum.* 14:225–250.
17. Lakowicz, J. R., H. Cherek, and A. Balter. 1981. Correction of timing errors in photomultipliers tubes used in phase and modulation fluorometry. *J. Biochem. Biophys. Methods.* 15:131–146.
18. Knopp, J. A., and J. W. Longworth. 1968. Energy transfer in oligotyrosyl compounds: fluorescence quenching as a function of the ionization of the phenolic hydroxyl groups. *Biochim. Biophys. Acta.* 154:436–443.
19. Prendergast, F. G., P. D. Hampton, and B. Jones. 1984. Characteristics of tyrosinate fluorescence emission in α- and β-purothionins. *Biochemistry.* 23:6690–6697.
20. Lakowicz, J. R., G. Laczko, H. Cherek, E. Gratton, and M. Limkeman. 1984. Analysis of the fluorescence decay kinetics from variable-frequency phase shift and modulation data. *Biophys. J.* 46:463–477.
21. Caceri, M. S., and W. P. Cacheris. 1984. Fitting curves to data. The simplex algorithm is the answer. *Byte.* May, 340–360.
22. Egami, F., K. Takahashi, and T. Uchida. 1964. Assay of Ribonuclease in Progress in Nucleic Acid Research and Molecular Biology, Vol. III. J. N. Davidson and W. E. Cohn, editors. Academic Press, New York. 59.
23. Bernstein, F. C., T. F. Koetzle, G. J. B. Williams, E. F. Meyer, Jr., M. D. Brice, J. R. Rogers, O. Kennard, T. Shimanouchi, and M. Tasumi. 1977. The protein databank: A computer based archival file for macromolecular structures. *J. Mol. Biol.* 112:535–542.
24. Hubbard, R. E. 1986. HYDRA: current and future developments. *In* Computer Graphics and Molecular Modeling. R. Fletterick and M. Zoller, editors. Current Communications in Molecular Biology, Cold Spring Harbor Laboratory.
25. Oobatake, M., S. Takahashi, and T. Ooi. 1979. Conformational stability in ribonuclease T1. I. Thermal denaturation and effects of salts. *J. Biochem.* 86:55–63.
26. Jameson, D. M., E. Gratton, and R. D. Hall. 1984. The measurement and analysis of heterogeneous emissions by multifrequency phase and modulation fluorometry. *Appl. Spectrosc. Rev.* 20:55–106.
27. Ludescher, R. D., J. J. Wolwerk, G. H. de Haas, and B. S. Hudson, 1985. Complex photophysics of the single tryptophan of porcine pancreatic phospholipase A2, its zymogen and an enzyme/micelle complex. *Biochemistry.* 24:7240–7249.
27a. Almassy, R. J., J. C. Fontecilla-Camps, F. L. Suddath, and C. E. Bugg. 1983. Structure of variant-3 scorpion neurotoxin from Centruroides scupturatus ewing, refined at 1.8 Å resolution. *J. Mol. Biol.* 170:497–527.
28. Krishna, N. R., C. E. Bugg, R. L. Stephens, and D. D. Watt. 1983. NMR studies of the variant-e neurotoxin from Centruroides sculpturatus ewing. *J. Biomol. Struct. & Dyn.* 1:829–842.
29. Howard, W. E., and E. W. Schalg. 1976. High resolution laser excitation on the low pressure gas: quantum yields of naphthaline. *Chem. Phys.* 17:123–138.
30. Engh, R. A., L. X.-Q. Chen, and G. R. Fleming. 1986. Conformational dynamics of tryptophan: a proposal for the origin of non-exponential fluorescence decay. *Chem. Phys. Lett.* 126:365–372.
31. James, D. R., and W. R. Ware. 1985. Multiexponential fluorescence decay of indole-3-alkanoic acids. *J. Phys. Chem.* 89:5450–5458.
32. Chang, M. C., J. W. Petrich, D. B. McDonald, and G. R. Fleming. 1983. Nonexponential decay of tryptophan, tryptophyglycine and glyciltryptophan. *J. Am. Chem. Soc.* 105:3819–3824.
33. Szabo A. G., and D. M. Rayner. 1980. Fluorescence decay of tryptophan conformers in aqueous solution. *J. Am. Chem. Soc.* 102:2, 554–563.
34. Petrich, J. W., M. C. Chang, D. B. McDonald, and G. R. Fleming. 1983. On the origin of nonexponential decay in tryptophan and its derivatives. *J. Am. Chem. Soc.* 105:3824–3832.
35. Laws, W. R., J. B. A. Ross, H. R. Wyssbrod, J. M. Beechem, L. Brand, and J. C. Sutherland. 1986. Time resolved fluorescence and H-NMR studies of tyrosine and tyrosine analogues: correlation of NMR-determined rotamer populations of fluorescence kinetics. *Biochemistry.* 25:599–607.
36. Ross, J. B. A., W. R. Laws, A. Buku, J. C. Sutherland, and H. R. Wyssbrod. 1986. Time resolved fluorescence and ^{1}H NMR studies of tyrosyl residues in oxytocin and small peptides: correlations of NMR-determined conformations of tyrosyl residues and fluorescence decay kinetics. *Biochemistry.* 25:607–612.
37. Prendergast, F. G., G. Ford, K. Ward, and J. Wick. 1985. Structure-luminescence correlation in proteins. *J. Cell. Biochem.* 9B (Suppl.): 136.
38. James, D. R., D. R. Demmer, R. P. Steer, and R. E. Verrall. 1985. Fluorescence lifetime quenching and anisotropy studies of ribonuclease T1. *Biochemistry.* 24:5517–5526.
39. Heinemann, U., and W. Saenger. 1982. Specific protein-nucleic acid recognition in ribonuclease T1-2′-guanylic acid complex: an x-ray study. *Nature (Lond.).* 299:27–31.
40. Eftink, M. R. and C. A. Ghiron. 1975. Dynamics of a protein matrix revealed by fluorescence quenching. *Proc. Natl. Acad. Sci. USA.* 72:3290–3294.
41. Eftink, M. 1983. Quenching-resolved emission anisotropy studies with single and multitryptophan-containing proteins. *Biophys. J.* 43:323–334.
42. Ricci, R. W. 1984. Inclusion complexes of cyclohexaamylose with indole. *Carbohydrate Res.* 129:278–288.
43. Ichiye, I., and M. Karplus. 1983. Fluorescence depolarization of tryptophan residues in proteins: a molecular dynamics study. *Biochemistry* 22:2884–2893.
44. Haycock, C., and P. G. Prendergast. 1986. A model of protein fluorescence incorporating chromophore interactions and dynamics. *Biophys. J.* 49(2, Pt. 2):62a. (Abstr.)
45. Liebman, M., and P. G. Prendergast. 1985. Correlation of protein structure and luminescence: use of molecular electrostatic potentials. *Biochemistry.* 24:3384.
46. Macgregor, R. B., and G. Weber. 1986. Estimation of the polarity of the protein interior by optical spectroscopy. *Nature (Lond.).* 319:70–73.
47. Connolly, M. L. 1983. Solvent-accessible surfaces of proteins and nucleic acids. *Science (Wash. DC).* 221:709–713.